Analysis of the Factors Determining the EPR Spectra of Spin Probes That Partition between Aqueous and Lipid Phases[1a]

Carl F. Polnaszek,[1b] Shirley Schreier,[1c] Keith W. Butler, and Ian C. P. Smith*

Contribution from the Division of Biological Sciences, National Research Council, Ottawa, Canada K1A 0R6. *Received November 3, 1977*

Abstract: Electron paramagentic resonance spectra of spin probes that partition between lipid and water were examined in water-phospholipid mixtures, fatty acids, and long-chain hydrocarbons. The concentrations of the probes in the phospholipid and aqueous phases were determined by several methods. Rigorous calculations of correlation times were performed. The analysis of the two parameters—concentration and correlation time in each phase—indicated that breaks in plots of partition parameters determined from measurements of line heights do not always reflect accurately the actual probe distribution in lipid-water phases, primarily as a consequence of the different activation energies for probe rotation in each phase. The delineation of the various processes underlying the spectra of partitioning molecules should allow a more reliable use of these probes in complex systems. Unresolved proton hyperfine splittings, ring interconversion, molecular ordering, probe location, and probe-probe interactions affect the spectral line shapes. The contribution of each factor depends upon the probe and the system. Neglect of ordering of the probes where this occurs leads to wrong evaluation of correlation times, and hence to erroneous values for the microviscosity.

I. Introduction

Spin probes that partition between a membrane environment and the aqueous phase surrounding it yield spectra that often have two resolved high-field components at normal X-band electron paramagnetic resonance (EPR) frequencies[2-10] (Figure 1). Such spectra have been analyzed in terms of the assumption that the *relative heights* of the two lines are proportional to the concentrations of the probe in the two media. The partition parameter,[2] f ($H/(H + P)$ in Figure 1), has been used for determination of liquid crystal-gel phase transition temperatures,[3] phase diagrams of lipid mixtures,[3] and temperatures for the onset and completion of lateral phase separations in biological membranes[3] and in the inner and outer monolayers of those membranes.[4] Lipid cluster formation at temperatures above the phase transition has been inferred from breaks in the plot of α (a parameter analogous to f, (H/P in Figure 1)) as a function of temperature.[9] Partitioning experiments have provided support for the existence of boundary lipid in an enzyme that spans a membrane.[10]

We have analyzed the line shapes of the EPR spectra of two spin probes, 2,2,6,6-tetramethylpiperidinyl-*N*-oxy (Tempo) and perdeuterated 4-oxo-2,2,6,6-tetramethylpiperidinyl-*N*-oxy (pd-Tempone), that partition between water and lipid in a series of systems.

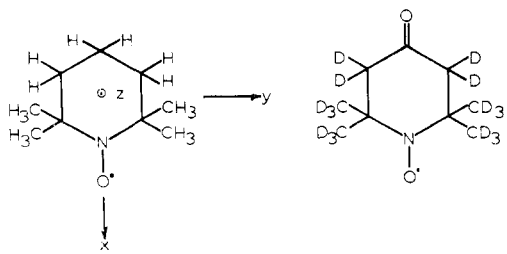

TEMPO pd-TEMPONE

The first probe has been employed in many of the earlier studies described above. Perdeuterated Tempone was used because its relaxation properties have been well studied[11,12] and because its EPR resonances are narrower than those of Tempo (Figure 1), making the measurement of the relative amplitudes of the hyperfine lines and deviations from symmetric line shapes more accurate. Tempone has also been employed in determination of the viscosity of membrane-water systems.[13] Our experiments were performed with phospholipid-water mixtures and with fatty acids, hydrocarbons, and aqueous solutions. Inorganic paramagnetic ions were added to phospholipid-water systems to remove the spectrum of the spin probe in aqueous solution.[13] Integrated intensities and spin concentrations were calculated to investigate the errors introduced into parameters f and α calculated by the use of peak heights (H and P, Figure 1).

The EPR spectra were analyzed in terms of the motional narrowing theory.[14,15] We find that the spectral features of partitioning spin probes are complex due to different rates of motion in the two environments, ordering of the probes in the lipid phase, and distribution and aggregation of the probes within the membrane. Changes in the packing of the lipid can also induce selective aggregation of the probes and broadening of the resonances.

II. Materials and Methods

Egg lecithin (EL) was obtained from Lipid Products Limited, dipalmitoyl lecithin (DPL) from General Biochemicals and Grand Island Biological Co., di-*tert*-butyl nitroxide (DTBN), octadecane, and decanoic acid from Eastman Organic Chemicals, *n*-decane from Phillips Petroleum, oleic acid (>99% pure) from Sigma Chemical Co., potassium ferricyanide and nickel sulfate from Anachemia, Nematic phase 7A from EM Laboratories, and paraffin oil ("Liquid Paraffin, Mineral Oil (Heavy)") from British Drug Houses. Tempo was synthesized by Dr. F. Hasan by the oxidation of 2,2,6,6-tetramethylpiperidine (Frinton Laboratories) as described by Rozantsev.[16] Perdeuterated Tempone (pd-Tempone) was synthesized by Dr. R. P. Mason from acetone-d_6 and ammonia-d_3 by the method of Rozantsev.[16] The 2',2'-dimethyloxazolidinyl-*N*-oxy derivative of 12-keto stearic acid (12-SASL) was purchased from Syva.

The aqueous buffer was made up of 5 mM 3-(*N*-morpholino)propanesulfonic acid (MOPS, Calbiochem) and 0.145 M NaCl; pH was adjusted to 7.4 with TRIZMA BASE [tris(hydroxymethyl)aminomethane, Sigma]. Chloroform solutions of the lipids were evaporated to dryness with a stream of N_2. Residual solvent was removed by evaporation under vacuum for at least 4 h, the lipid was dispersed in aqueous buffer by vigorous shaking, and Tempo and pd-Tempone (5×10^{-3} M in buffer) were added. To prepare samples of pure organic compounds a chloroform solution of the probe (2.5 M) was evaporated with a stream of dry N_2 and the fluid solvent added. The spin probe concentration in all samples was $\leq 5 \times 10^{-4}$ M.

Sonication of phospholipid-water systems at temperatures above the phase transition was continued until a clear suspension was obtained (about 20 min) in a Cole Parmer Model 8845-3 ultrasonic cleaner. NMR spectra were taken with Varian CFT-20 (^{13}C) and EM

0002-7863/78/1500-8223$01.00/0 Published 1978 American Chemical Society

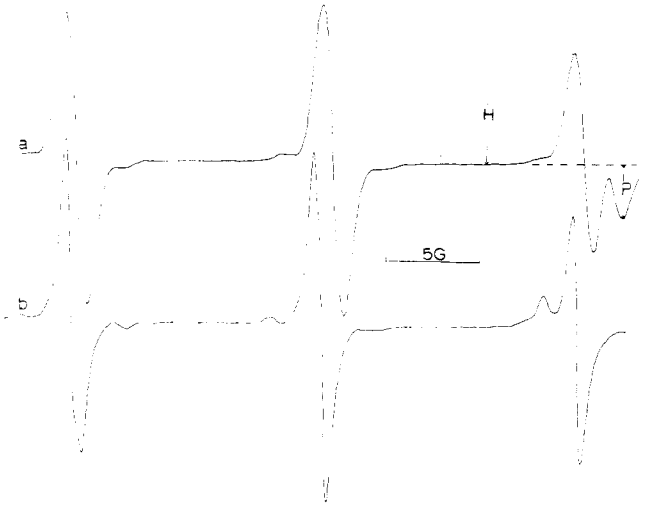

Figure 1. Spectra of spin probes in EL dispersions in buffer: (a) Tempo, T = 35.5 °C, 11% lipid (weight); (b) pd-Tempone, T = 33.4 °C, 20% lipid. The peak amplitudes labeled H (probe in lipid) and P (probe in water) are used to calculate $f = H/(H + P)$ and $\alpha = H/P$.

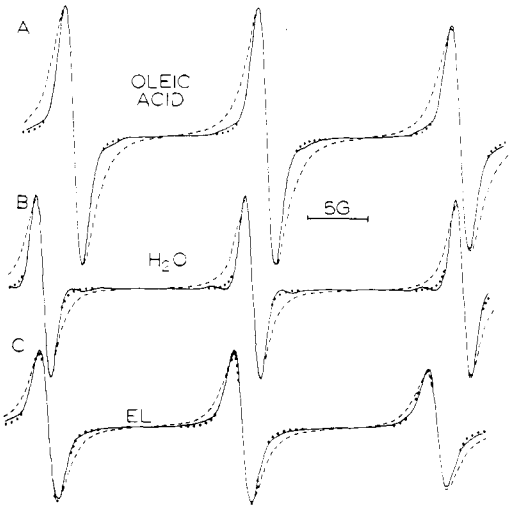

Figure 2. Spectra of Tempo in (A) oleic acid at 21.8 °C, (B) in buffer at 21.3 °C, and (C) in EL in the presence of 0.125 M Ni^{2+} at 23.7 °C: (—) experimental spectra; (- - -) theoretical spectra using Lorentzian lines, the measured line width of the center peak and line height ratios; (···) theoretical spectra including proton hyperfine splittings (hfs). In A and C the proton hfs values of ref 24a were used. In B the values determined by best fit a_{CH_3} = 0.17 G and a_{CH_2} = 0.42 G were used.

360 (^{1}H) spectrometers. Viscosities were determined using an Ostwald viscometer.[17] EPR spectra were obtained using a Varian E9 X-band spectrometer. Double integration of spectra was accomplished by means of a Varian 620I computer with program 994002-00A. All variable temperature experiments were started at the highest temperature.

Oriented multibilayers were prepared as described previously.[18] Dispersions of lipids or aqueous samples were studied in low temperature aqueous solution sample cells (Scanco) which were calibrated among themselves using a standard sample for concentration measurements. For nonlossy solvents, 5-mm NMR tubes were used. In some experiments one or two narrow (<1 mm o.d.) capillaries were attached to the low-temperature aqueous cells to investigate two-component systems and to determine hyperfine splittings and g values. As standards we used Fremy's salt (PADS),[15] DTBN,[8a] and pd-Tempone (a_N = 16.17 G[19] and g = 2.00560) in aqueous solutions.

Integrated Intensities. The total spin probe concentration (in arbitrary units) can be described as

$$[\text{spin probe}]_{\text{total}} = [\text{spin probe}]_{\text{lipid}} + [\text{spin probe}]_{\text{aq}} \quad (1)$$

and can be calculated from double integration of the spectra. The fraction of probe in the aqueous environment was calculated according to the following: (1) It was assumed that the bottom half of the second high-field resonance (P in Figure 1) in the spectra of dispersions was due solely to probe in water.[20] (2) Spectra of the probe at a known concentration in aqueous solution yielded a value P' for the height of the bottom half of the high-field resonance and a value A'_{H_2O} for the second integral. Then, if P and P' are normalized to the same spectrometer settings, $[\text{spin probe}]_{aq}$ in the lipid dispersion can be calculated according to:

$$[\text{spin probe}]_{aq} = (P/P') \times A'_{H_2O} \quad (2)$$

The concentration of probe in lipid was calculated by subtracting the value obtained from eq 2 from the total spin probe concentration (see Cannon et al.[21]). Another procedure has been presented by Castle and Hubbell.[22]

Calculation of Correlation Times. Spectra were analyzed in terms of the motional narrowing theory[14,15] as applied previously to spin probes in membrane systems by Cannon et al.[21] The residual line widths ΔH were determined from each spectrum, correcting for inhomogeneous broadening as described below.[11] The line widths of the individual hyperfine resonances are given by

$$\Delta H_m = A + Bm + Cm^2 \quad (3)$$

where m is the z component of the nitrogen nuclear spin quantum number. For isotropic motion the line width coefficients B and C (in gauss, peak-to-peak) are dependent upon the correlation time τ in the following manner[15]

$$B = 0.103\omega_0[\Delta g\Delta a + 3(\delta g)(\delta a)] \times \tau[1 + \tfrac{3}{4}(1 + \omega_0^2\tau^2)^{-1}]$$
$$C = 1.81 \times 10^6[(\Delta a)^2 + 3(\delta a)^2] \times \tau[1 - \tfrac{3}{8}(1 + \omega_a^2\tau^2)^{-1} - \tfrac{1}{8}(1 + \omega_0^2\tau^2)^{-1}] \quad (4)$$

where

$$\Delta a = a_z - \tfrac{1}{2}(a_x + a_y) \text{ and } \delta a = \tfrac{1}{2}(a_x - a_y) \quad (5)$$

with the a's in gauss, $\omega_a \simeq 8.8 \times 10^6\, a_N$, where a_N is the isotropic hyperfine splitting, $\omega_0 = 2\pi\nu_0$, where ν_0 is the spectrometer frequency, and x, y, and z are the principal axes of the nitroxide. Quantities Δg and δg are defined similarly to Δa and δa. The line-width coefficient A is also dependent upon Heisenberg exchange and dipolar broadening and can be used as an indication of the presence of these phenomena. Correlation times were calculated using eq 4. We denote the τ's calculated from the B and C coefficients as τ_B and τ_c, respectively.

Whenever a single three-line spectrum was obtained (see Results) the experimental line shapes for Tempo were non-Lorentzian. This could be due to slow motional effects,[11,12,15,21,23] but this is an unlikely explanation as the calculated values of the correlation times τ were $\leq 10^{-9}$ s at temperatures above 0 °C. Unresolved proton hyperfine splittings can account for the observed non-Lorentzian line shape (Figure 2), yielding the correct line shape in the wings, and are important when considering the overlap of two spectra. The line-width coefficients A, B, and C were determined using the obtained values of the proton or deuteron splittings in the usual manner.[11,15,25,26]

Order parameters were calculated from the measured hyperfine splittings and g values of oriented multibilayers.[11b] The values of a_z (Table I) and g_z were determined from spectra obtained at low temperatures ($T < -140$ °C).

III. Results

Values for the partition coefficients between n-decane and buffer of Tempo and pd-Tempone and of 12-SASL[21,27] and DTNB[5,8a] are given in Table II. Hyperfine splitting constants and g values for the systems studied in this work are given in Table I. The quantities g_x, g_y, a_x, and a_y needed to calculate correlation times[11,12,14,15] could only be determined for pd-Tempone in paraffin oil by simulation of the polycrystalline rigid limit spectra[11,15] (g_x = 2.00985, g_y = 2.0063, g_z = 2.0021, a_x = 5.5 G, and a_y = 5.3 G). For the other systems it was assumed that $a_x = a_y = (3a_N - a_z)/2$ and g_x and g_y were adjusted to give the proper isotropic value of g.

Table I. Magnetic Parameters for Tempo and pd-Tempone

system	Tempo			pd-Tempone		
	a_N, G	a_z, G	g	a_N, G	a_z, G	g
water	17.33	38.1	2.005 58	16.17	36.6	2.005 60
20% glycerol-water	17.2	37.7	2.005 66	16.18	36.45	2.005 62
glycerol	16.76	37.5				
egg lecithin	15.96	36.5	2.006 08	15.05	34.1	2.005 99
DPL[a]	15.97	35.7		15.04	34.2	
decanoic acid[a]	16.00	36.6		14.94	34.9	
oleic acid[a]	16.00	36.3	2.006 09	14.80	34.2	2.006 00
phase 7-A[a]	15.64	33.9		14.76	33.4	2.006 01
octadecane[a]	15.40			14.48		
paraffin oil	15.44	33.3	2.006 15	14.46	32.5	2.006 08

[a] a_N and g were determined above the phase transition temperature.

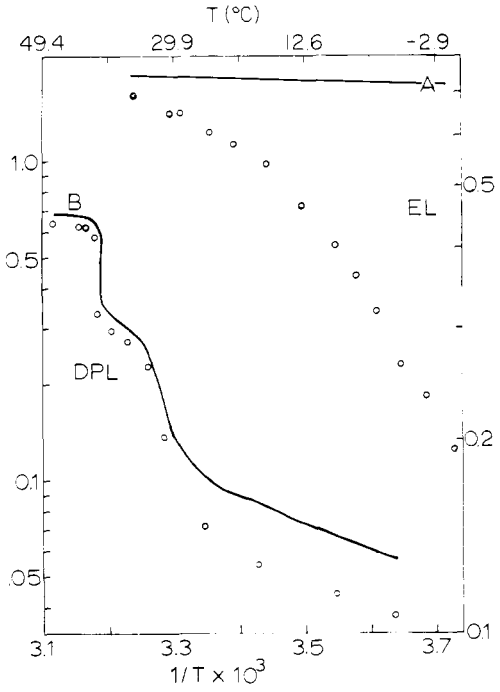

Figure 3. The ln f vs. $1/T$ for Tempo in phospholipid dispersions (○). The ln of fraction of spin probe in lipid as determined by the method of integrated intensities is given by the solid lines: (A) EL dispersions (11% by weight), right-hand scale; (B) DPL dispersions (9% by weight), left-hand scale.

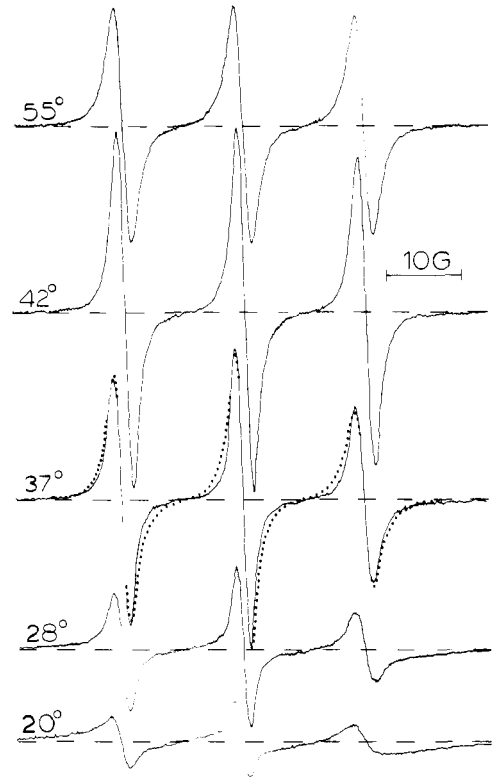

Figure 4. Spectra of Tempo in DPL dispersions as a function of temperature in the presence of 0.125 M Ni^{2+}. The spectrometer settings were the same for all spectra: microwave power, 10 mW; modulation amplitude, 1 G; receiver gain, 2×10^3; scan range, 100 G in 500 s; time constant, 0.3 s. An attempt was made to fit the 37 °C spectrum theoretically (···) using the proton splittings of ref 24a and the appropriate *A*, *B*, and *C* parameters determined from the relative peak heights and the line width of the central peak.

Table II. Partition Coefficients between Decane and Buffer (pH 7.4) for the Probes Used in the Present Work at Room Temperature (23 ± 2 °C)

probe	vol partition coeff	
	n-decane/ buffer	DPL/ buffer[a]
Tempo	28	26
pd-Tempone	0.9	2.6[b]
12-SASL	42	
DTBN	52	22

[a] at 50 °C, ref. 5e; [b] Tempone.

A. Phospholipids. Figure 1 shows the spectra of Tempo and pd-Tempone in dispersions of EL. The resonances in the spectra of pd-Tempone were much narrower due to the absence of unresolved proton hyperfine splittings.

Plots of ln f vs. $1/T$ for Tempo in EL and DPL dispersions are shown in Figure 3. We obtained similar results by plotting f vs. T and ln α vs. $1/T$, as reported by Gaffney.[28] A comparison of the temperature dependence of the f values and of the fraction of the spin probe in lipid determined by double integration for Tempo in phospholipids is given in Figure 3. A good parallel is obtained in the case of DPL, in which we observe both the main transition at 40.7 °C and the pretransition at 32.5 °C, but not with EL. Thus, the partitioning of the probe between two environments is not always the main factor determining the value of f.

Effect of Paramagnetic Ions. In aqueous dispersions of lipids, the EPR spectra of nitroxide probes in the aqueous phase are broadened beyond detection by 0.125 M Ni^{2+} or ferricyanide[13,29] (Figure 4). Some line broadening in the remaining spectrum is observed in both systems, more for single bilayer vesicles than for dispersions. The broadening is proportional to the concentration of paramagnetic ions and is less when the ions are added to a lipid dispersion than when they are present in the solution used to form the dispersion. This broadening

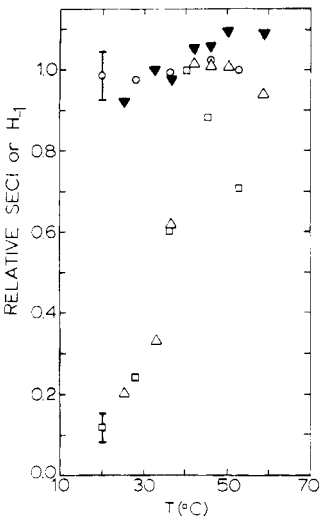

Figure 5. The relative total integrated intensity (SECI) for (▼) Tempo in DPL and (○) Tempo in DPL in the presence of 0.125 M Ni^{2+} as a function of temperature. The relative amplitude of the H peak (see Figure 1) for (△) Tempo in DPL and (□) Tempo in DPL in the presence of Ni^{2+} as a function of temperature. The lipid concentration was 9% by weight for both samples.

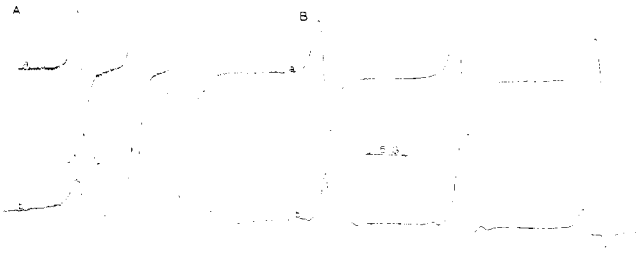

Figure 6. Spectra of Tempo (a) and pd-Tempone (b) in EL (A) and DPL (B) in the presence of 0.125 M Ni^{2+} at 25 °C. Note the change in sweep width from A to B.

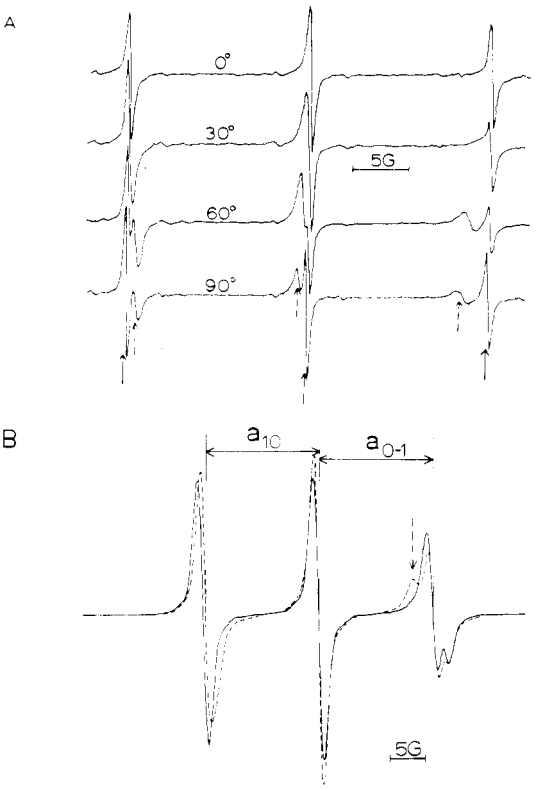

Figure 7. (A) Spectra of pd-Tempone in egg lecithin planar multibilayers at angles of 0, 30, 60, and 90° between the bilayer normal and the applied magnetic field. (B) Spectra of Tempo in EL planar multibilayers: (- - -) parallel (0°); (—) perpendicular (90°). The solid arrows indicate lines due to probe primarily in the aqueous phase; the dashed arrows indicate lines due to probe in the lipid phase. $a_{1,0}$ is the separation between the low-field line and the center line, measured at the base line; $a_{0,-1}$ is the separation between the center line and the high-field line, measured at the base line. All spectra taken at room temperature (22 ± 2 °C).

is presumably due to a paramagnetic interaction between the ions and the probes near or at the aqueous interface, which persists for a time of the order of $T_1 \approx 10^{-6}$ s.[12] Mg^{2+} (which has approximately the same radius[30] as Ni^{2+}) was used as a control for the possible effects of Ni^{2+} on membrane structure.[31] In the presence of Mg^{2+} the main transition temperature of DPL was changed by +1 °C and f was decreased by 30 to 65% compared to the values in Figure 3 as the temperature decreased (below the transition).

Calculation of Probe Concentration. The concentrations of Tempo in the lipid phase of DPL calculated as a function of temperature (Figure 5) from the double integrals of the spectra in Figure 4 were not in agreement with those obtained in the absence of Ni^{2+} (Figure 3). Figure 5 shows that as the temperature changed, the probe concentration remained nearly constant. This could be due to increasing permeability of the lipid to paramagnetic ions with increasing temperature such that the resonances due to some probes in the membrane are broadened beyond detection, or that at higher temperatures, a larger proportion of the probe in the membrane spends, on the average, longer times close to the membrane-water interface, thus becoming more available for interactions with the aqueous paramagnetic ions. These effects will persist for a time T_1, the spin-lattice relaxation time of the nitroxide, in the membrane itself. A similar result[13d] was obtained from Tempone in dimyristoyllecithin (DML) in the presence of Ni^{2+}.

In a separate experiment we observed a considerable loss (about 75% at room temperature) of the integrated signal intensity expected for Tempo in DPL in the presence of 0.125 M paramagnetic broadening agents. This, in conjunction with the variable temperature study, leads to the conclusion that a large proportion of the probe in lipid is unobservable in the presence of paramagnetic ions, and therefore that one cannot accurately calculate the probe concentration by this method.

Line Shapes. In the presence of paramagnetic ions several of the line shapes (Figure 6) are not symmetric, as was the case in Figure 2. This asymmetry can be measured by r_m, the ratio of the positive to the negative part of the derivative amplitude of the mth line. Deviations of r_m from unity indicate that the probes in the lipid may be ordered and/or rotating slowly ($\tau > 10^{-9}$). The spectra of pd-Tempone are not characteristic of this probe rotating at a slow rate.[11] Ordering is a measure of the distribution of probe orientations with respect to the bilayer normal and will cause the hyperfine splitting to vary with orientation.[3,11,18]

Planar Multibilayers. To test for molecular ordering, spectra were run of the probes in oriented planar multibilayers of phospholipids[18] as a function of the angle between the bilayer normal and the applied magnetic field (Figure 7). The orientation dependence of the spectra due to the ordering of the probe is especially evident for pd-Tempone, Figure 7A, in both the hyperfine splitting and line shape. The spectra at 90 °C, and to a lesser extent at 60 °C, display resolution of all three resonances for the probes in the lipid and aqueous phases. The spectra of the probes in the aqueous phase are independent of orientation, as expected.

Table III. Parameters Measured and Calculated from Figure 7 for the Spectra of Tempo and pd-Tempone in Egg Lecithin Planar Multibilayers[f]

probe	angle[g]	$a_{1,0}$, G	$a_{0,-1}$, G	h_1	h_{-1}	r_1	r_0	r_{-1}
Tempo	0	16.0	16.2	0.766	0.377[a]	1.274	0.922	0.949[a]
	90	16.4	16.0	0.933	0.485[a]	1.028	0.926	1.426[a]
Tempo[d]	0	16.1	16.2	0.922	0.618	1.156	1.094	1.098
	90	16.1	16.1	1.004	0.790	0.936	1.022	1.292
Tempo	H_2O[e]	17.3	17.4	1.003	0.964	1.059	1.059	1.073
pd-Tempone	0	16.2	16.3	0.862	0.725[a]	0.942	0.866	0.965[a]
	30	16.2	16.2	1.051	0.503[a]	1.454	0.616	0.561[a]
	60	15.0	14.9	0.745	0.385[b]	4.513	0.687	0.586[b]
					0.156[c]			1.727[c]
	90	14.7	14.7	1.184	0.773[b]	1.360	0.573	0.898[b]
					0.098[c]			1.034[c]
pd-Tempone[d]	0	15.96	16.12	0.951	0.541	1.037	0.966	0.690
	90	14.76	14.68	0.980	0.654	1.006	1.022	1.093
pd-Tempone	H_2O[e]	16.2	16.2	1.003	0.811	1.032	1.021	1.020

[a] The data here refer to the line with greater amplitude. [b] Data for the line due to aqueous phase. [c] Data for the line due to lipid phase. [d] In the presence of Ni^{2+}. [e] Probe in isotropic H_2O. [f] The parameters are defined in the figure and in the text. [g] Angle between bilayer normal and applied magnetic field.

The ordering of pd-Tempone is in agreement with results for a nonpolar nematic phase (phase 7A), where the relative degrees of order found follow: pd-Tempone, 1; Tempo, 0.7; DTBN, 0.3.[11b] In the presence of Ni^{2+} the relative order of the first two probes in EL is considerably different, ca. 15:1.

Table III lists a series of parameters measured and calculated from Figure 7. Splittings $a_{1,0}$ and $a_{0,-1}$ were measured as indicated in Figure 7B; h_1 and h_{-1} are the relative amplitudes of the low- and high-field lines normalized with respect to the center line ($h_0 = 1.000$). Deviations from expected values can be interpreted as due to contribution of more than one type of spectrum to the overall line shape[15b] and also of different relative motions in the two phases. Thus, deviations of r's from unity, as well as deviation of the relative amplitudes (h's) of the outer lines from the values in water, were ascribed to the presence of several subspectra. The behavior of the h parameters and the different line widths for the high-field lines in the 90 °C spectrum (Figure 7A) were taken as an indication of different relative motions in the lipid and aqueous phase.

Spectral Simulations and Correlation Times. Tempo in all systems yields three-line spectra, or a superposition of these, allowing the calculation of correlation times using motional narrowing equations. One can try to fit experimental spectra such as those in Figure 1 by summing theoretical spectra determined from the calculated single-component spectra. This procedure is only feasible in the absence of ordering. The degree of ordering of Tempo is low (Figure 7B) and, if neglected, will affect the observed line shapes only to a small extent (Figure 2C).

The values of the A line width coefficients (eq 3), obtained after correcting for the proton splittings as in Figure 2, are comparable for the two probes Tempo and pd-Tempone. The A coefficients also allow the evaluation of exchange or dipolar broadening on the spectra of the probes (vide infra).

Further improvement of the simulations is obtained by including the ^{13}C hyperfine splittings which give rise to the satellites seen in the experimental spectra. This was done in attempts to simulate the experimental spectra in the phospholipid–water system. Next the intrinsic line widths were calculated and thence values of τ_B and τ_C for Tempo in all systems and for pd-Tempone in only the nonordered pure solvents. We found that $\tau_C > \tau_B$ in many cases. This could result in the line-shape asymmetry seen in Figure 6 and will be dealt with in Analysis and Discussion. We have used τ_B as an indicator of the motional characteristics of Tempo in phospholipids.

The behavior of $\ln \tau_B$ vs. $1/T$ (Figure 8) can be compared to that of $\ln f$ vs. $1/T$ (Figure 3). Sharp breaks occur for DPL

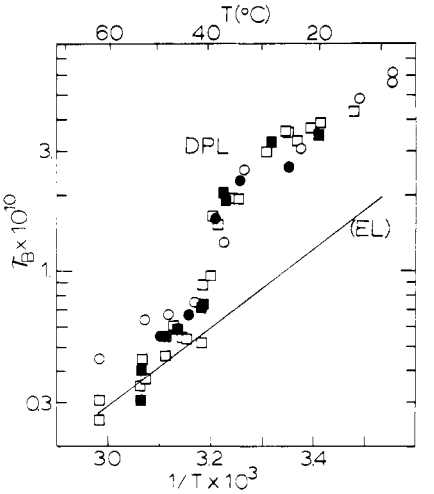

Figure 8. Logarithm of deduced τ_B values versus $1/T$ for Tempo in phospholipid systems in the presence of paramagnetic ions. (—) EL dispersions, containing either Ni^{2+} or ferricyanide. Individual points are for DPL with (□) Ni^{2+} or (○) ferricyanide added to prepared dispersions, (■) the Ni^{2+} solution used to prepare the dispersions, and (●) ferricyanide added to prepared dispersions before sonication.

in both plots (40.7 °C for f and 39.1 °C for τ_B). However, the change in slope for f seen for EL at ~13 °C is absent for τ_B.

To obtain τ's from the spectra of pd-Tempone in phospholipids (Figure 6), it is necessary to use a method which includes an order parameter as a variable.[11b-d,32] This was not attempted, but we note that an error will be introduced in the calculation of microviscosity of phospholipid media using the assumption that the motion is isotropic.

In summary, with the phospholipid–water systems we have examined the effects on the spectra of the probes Tempo and pd-Tempone of (a) temperature in dispersions, (b) paramagnetic ions in dispersions, and (c) orientation in planar multibilayers. Calculation of the probe concentration in the lipid phase and analysis of the line shapes (see Analysis and Discussion) enables one to determine the contribution to the ratio of the high-field line heights of factors other than partitioning. Differential line broadening in the spectra of Tempo in the lipid and aqueous phases taken as a function of temperature introduces errors in the calculation of f parameters.

B. Long-Chain Compounds and Water. Ideally one would like to be able to reconstruct the spectra of spin probes partitioning between lipids and water as being due to the sum of two

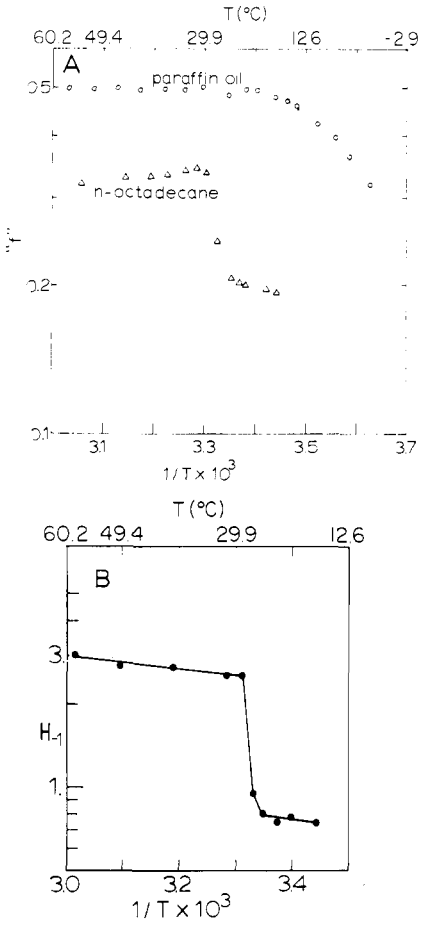

Figure 9. (A) Logarithm of the deduced f parameter obtained from the composite spectra of Tempo in (○) paraffin oil-buffer and in (△) *n*-octadecane-buffer (run in separate tubes, see Materials and Methods) as a function of $1/T$. (B) Logarithm of the height (H_{-1}) in arbitrary units of the high-field peak of the spectrum of Tempo in octadecane as a function of $1/T$.

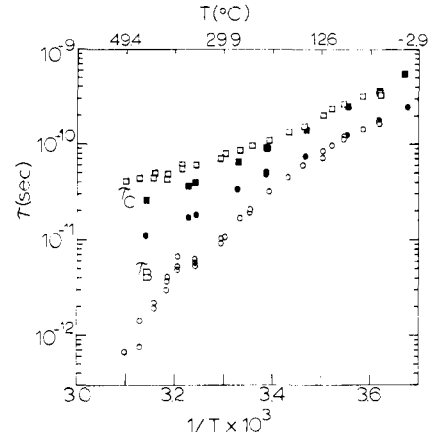

Figure 10. Logarithm of the deduced values of τ_B (circles) and τ_C (squares) for Tempo (open symbols) and pd-Tempone (filled symbols) in paraffin oil as a function of $1/T$.

distinct spectra. One method of obtaining the spectrum in lipid—eliminating the signal from the aqueous phase by means of inorganic paramagnetic broadening agents—was considered above. We also examined the spectra of the probes in water and in systems containing long acyl chains from which only one spectrum is obtained. These were paraffin oil, octadecane, oleic acid, and decanoic acid.

Solutions of the probe in water and in a long-chain compound, in two separate tubes, were placed inside the EPR cavity. The composite spectra resembled those of the phospholipid dispersions (Figure 1). The apparent f parameter was calculated and plots of ln f vs. $1/T$ gave large breaks at a temperature close to the melting point of the long-chain compounds. Results are shown in Figure 9A for Tempo in octadecane. Evidently, no change in partitioning occurs and the change in f is due to a change in the spectrum of the probe in octadecane. This can be seen from Figure 9B where ln H_{-1} vs. $1/T$ is plotted for the spectra of the probe in octadecane alone. In the case of paraffin oil-water a change in slope in the plot of ln f vs. $1/T$ occurred at ~15 °C (Figure 9A), whereas paraffin oil alone displayed a break at ~20 °C in the plot of ln H_{-1} vs. $1/T$. A sharp phase change does not occur since paraffin oil consists of a mixture of branched hydrocarbons (of different length) as shown by its ^{13}C and ^{1}H NMR spectra.

To delineate the phenomena responsible for these breaks, we determined the line-width coefficients, correcting for proton broadening, as shown in Figure 2 and calculated τ_B and τ_C (eq 4). No long-range ordering had to be included. The results for the two probes in paraffin oil are shown in Figure 10. For compounds with well-defined melting points, changes in the slope of such plots, but not sharp breaks, were observed near the melting temperatures using pd-Tempone. For the fatty acids we found no change in slope for Tempo. The A line-width coefficient (see eq 3) did exhibit sharp breaks at the melting points of *all* compounds investigated with *all* spin probes, due to enhanced spin-spin interactions[13,29,34] (Heisenberg exchange or electron dipolar broadening) resulting from aggregation of the probe below the melting point.[35] This broadening is largely responsible for the sharp breaks in Figure 9.

Plots of ln τ vs. $1/T$ allowed the determination of the melting points, activation energies, and other physical parameters (Table IV). Table I shows that the magnetic parameters for Tempo in the fatty acids are nearly the same as those from the spectra obtained from phospholipid dispersions in the presence of inorganic paramagnetic ions. This and the inequality of the calculated τ's ($\tau_C \neq \tau_B$) will be considered in the next section.

IV. Analysis and Discussion

In the Results section data were presented in terms of integrated intensities, the f parameter, and correlation times. We shall now describe in greater detail the analysis we have performed on the spectra. Because all motions were rapid, we used the motional narrowing theory.[15] Table V presents the resultant τ values and those calculated using the Debye equation and the known viscosity. The lower values of the former are predicted by the Wirtz theory[11b] when the probe molecules are much smaller than those of the solvent, as is the case here.

The Effect of τ upon f. The values of τ_B for Tempo in the two phospholipid systems (Figure 8), determined in the presence of paramagnetic ions, are independent of the particular ion and of its concentration. For EL (no phase transition above the freezing point of water), the values of τ_B show no breaks or curvature as a function of temperature. The activation energy for rotation of Tempo is greater in EL than in water, and the deduced value of τ is about an order of magnitude larger in EL than in buffer at room temperature. Thus, the high-field line of Tempo in EL should broaden with decreasing temperature to a much greater extent than that of Tempo in water, causing f to vary in a nonlinear way, as seen for EL-water (Figure 3). Hence, effects ascribed to changes in slope of the parameters f and α such as lipid clustering[9,28] or multiple phase changes[4] may occur as a result of the differential line broadening of probes in the lipids and in the aqueous phase.[36]

For Tempo in DPL there is a sudden break in the deduced value of τ_B and τ_C unlike that observed for any of the other systems, yielding transition temperatures of 39.1 and 36.6 °C

Table IV. Characteristic Transition Temperatures and Activation Energies for the Systems Studied in This Work

compd	ref	parameter	probe[a]	E^{l}_{act},[b] kcal/mol	E^{s}_{act},[c] kcal/mol	transition,[d] °C
paraffin oil	this work	τ_B	II	11.7		
		τ_C	II	11.6		
		interconversion	I	3.6		~20
		f	I			~15
		H_{-1}	I			~20
octadecane	this work	τ_B	II	11.5	38	28.7
		τ_C	II	4.6	30	29.9
		f	I			28
		H_{-1}	I			28
	33	freezing point				28.2
decanoic acid	this work	τ	II	4.3	13.2	30.1
		τ	I	4.1		(not seen)
		f	I			30
		H_{-1}	I			30
	46	freezing point				31.4
oleic acid	this work	τ	I	6.1		(not seen)
		τ	II	6.9	2.4	4.2
	46	freezing point				4
EL	this work	τ	I	7.7		<−4
		f	I			~13
	5c	τ	DTBN	6.8		
	5c	f	DTBN			−9
	42	fluorescence[e]	DPH	8.3		<4
DPL	this work	f	I[f]			40.7
		τ_B	I[f]	7.5		39.1
		τ_B	I[g]	4.8		36.6
	2	f	I[f]			40.5
	44	f	I[g]			36.5
	42	fluorescence	DPH[f]	12.5		41.1
	42	fluorescence	DPH[g]	12.3		36.4
	45	DSC[f]				41.2
	45	DSC[g]				36.9
H_2O	this work	τ	I	4.8		
	this work	τ	II	4.0		

[a] I, Tempo; II, pd-Tempone; DPH, 1,3,5-diphenylhexatriene. [b] Activation energy in the liquid phase. [c] Activation energy in the solid phase. [d] Transition deduced from a change in slope is represented by an approximate sign. [e] In 1-palmitoyl-2-oleoylphosphatidylcholine, POPC. [f] In multilamellar dispersions. [g] In vesicles.

Table V. A Comparison of the Rotational Correlation Times (τ) Determined from Equation 4 with Those Calculated from the Debye Equation

compd	probe[a]	T, °C	τ_B[b]	τ_C[b]	τ_{Debye}[c]
paraffin oil	I	25	2.0×10^{-11}	9.5×10^{-11}	2.2×10^{-9}
	II		3.7×10^{-11}	7.6×10^{-11}	
octadecane[d]	II	40	3.4×10^{-12}	1.2×10^{-11}	9.1×10^{-11}
oleic acid	I	25	4.0×10^{-11}	4.1×10^{-11}	5.2×10^{-10}
	II		6.5×10^{-11}	6.0×10^{-11}	
H_2O[d]	I	25	1.0×10^{-11}	1.0×10^{-11}	4.1×10^{-11}
D_2O[e]	II	25	1.6×10^{-11}	1.7×10^{-11}	5.0×10^{-11}
EL[f]	I	25	1.0×10^{-10}	1.2×10^{-10}	2.0×10^{-9}
DPL[g]	I	50	4.5×10^{-11}	5.6×10^{-11}	8.6×10^{-10}
		25	3.5×10^{-10}	6.3×10^{-10}	5.1×10^{-8}

[a] I, Tempo; II, pd-Tempone. [b] Calculated from eq 4. [c] A molecular radius of 0.35 nm was used. [d] Viscosity from ref 33. [e] Viscosity from A. I. Kudish and D. Wolf, *J. Phys. Chem.*, **79**, 272–275 (1975). [f] Viscosity of POPC from ref 45. [g] Viscosity from ref 45.

for multilamellar dispersions and single bilayer vesicles, respectively (Table IV). The so-called pretransition[2] could not be detected. The large change in the apparent τ_B at the phase transition and the concomitant decrease in the amplitude of the high-field line due to probe in lipid (Fig. 4) will result in a large decrease in f upon going below the phase transition. Attempts to quantify this effect by line-shape simulation were not successful because of the presence of more than one component in the "lipid" spectra below the phase transition, resulting in line-shape asymmetry. The 37 °C spectrum in Figure 4 shows a comparison with the expected one-component spectrum simulated using proton splittings appropriate for above the phase transition.

Physical Interpretation of the τ Values. The τ values at 25 °C increase in the order octadecane < paraffin oil < decanoic acid < oleic acid < EL < DPL, and $\tau_C > \tau_B$ in most of the systems. We shall now discuss the physical processes that determine these results.

Effect of Intramolecular Interconversion. Both Tempo and pd-Tempone can exist in several rapidly interconverting conformations, characterized by either different ring conformers or the direction of the N–O bond.[24] When the rate of these processes becomes comparable to that for overall rotation, it can affect the relaxation properties of the system,[11a] and the coefficients B and C do not depend solely upon rotational processes as assumed in eq 4. We propose that this mechanism

is responsible for the differences between the activation energies calculated from τ values for Tempo and pd-Tempone in different systems (Table IV). The deduced τ values for pd-Tempone in paraffin oil are expected to be determined solely by overall rotation. For this probe the rate of ring or bond interconversion contributes to the line-width parameters only at very short τ values;[11a] this is apparent in the much less viscous[33] solvent octadecane, leading to different E^{1}_{act} values calculated from τ_B and τ_C (Table IV). Although $\tau_C \sim 2\tau_B$ in paraffin oil at all temperatures, the activation energies for rotation are 11.7 ± 0.2 and 11.6 ± 0.2 kcal/mol for τ_B and τ_C, respectively. The inequality $\tau_B < \tau_C$ results from short-range ordering (see below).

The values of τ for Tempo in paraffin oil at higher temperatures (>20 °C) are different from those for pd-Tempone. It is suggested that this is due to intramolecular interconversion of Tempo. Assuming that the τ_B values for pd-Tempone are the true *rotational* values for Tempo, we can estimate the τ value for ring or nitroxide interconversion in Tempo from the difference between the τ values for the two probes. Thence, the calculated E_{act} for interconversion is 3.3 ± 1.3 kcal/mol (Table IV). Therefore, the break in the f parameter (at ca. 15 °C) for composite spectra of Tempo in paraffin oil and in water can be ascribed solely to the change in relaxation of Tempo itself. Above this temperature the line widths of Tempo in paraffin oil depend upon *rotation* and *intramolecular interconversion,* whereas below this temperature they depend primarily upon rotation.

For Tempo in phospholipids, the calculated τ values were longer than in paraffin oil (Figure 10) and are in the range where the τ values for pd-Tempone and Tempo in the latter were essentially equal. Therefore, the nitroxide interconversion would not be expected to affect the τ values obtained in phospholipids.

For Tempo and pd-Tempone in the fatty acid model systems, the calculated values for τ_B and τ_C were nearly equal and the small differences could be reconciled by cancellation of the effects of probe interconversion or fluctuating torques (non-Brownian motion) ($\tau_C > \tau_B$)[11] with those of slightly anisotropic motion about the nitroxide x axis ($\tau_C < \tau_B$).[15]

Effect of Distribution of Probe Solubility and Short-Range Ordering. Asymmetric resonances were obtained for Tempo (Figure 4) and pd-Tempone in DPL in the gel phase, which could be due to ordering[21] and/or overlap of several spectra due to the probe in different environments with considerably different mobilities. The spectra can be simulated satisfactorily by considering slow exchange between different membrane sites, and also yield $\tau_C > \tau_B$.

It was also observed that $\tau_C > \tau_B$ for both probes in paraffin oil and in octadecane above the melting point. However, here the resonances were symmetrical. Despite the absence of long-range order, alkanes exhibit short-range ordering,[37] i.e., the chains are likely to be parallel for a short time ($\leq 10^{-7}$ s). Fluctuation of this short-range ordering has been postulated as a relaxation mechanism and a simple analysis has shown that $\tau_C > \tau_B$ for this mechanism.[11b,c]

Effect of Anisotropic Motion. In this case, for simplicity, we can assume that the rotation is characterized by two parameters, $\tau_{\parallel}$ and $\tau_{\perp}$ (the calculated τ's for rotation about and perpendicular to a principal axis, respectively). The ratio $\tau_{\perp}/\tau_{\parallel}$ yields the anisotropy ratio.[15] The ratio of τ_C/τ_B (calculated from the formalism for isotropic motion[15]) will indicate the preferential axis about which rotation takes place. For $\tau_C/\tau_B > 1$, it will be the y axis. For pd-Tempone in paraffin oil $\tau_C \simeq 2\tau_B$ (Figure 10), yielding an anisotropy ratio of 6.4 ± 0.9. This seems unreasonable for pd-Tempone in view of its nearly spherical shape and the absence of strong interactions with the paraffin solvent, providing further support for the explanation invoked in the previous section for $\tau_C \simeq 2\tau_B$ in paraffin oil, namely short-range ordering.

Order Parameters. The motionally averaged splittings and g values measured from Figure 7A were used to calculate the spectra (Figure 6B) in the lipid dispersions and to determine the ordering tensor[11] for pd-Tempone in EL: $S_{xx} = -0.043$, $S_{yy} = -0.023$, and $S_{zz} = +0.066$. The positive value of S_{zz} indicates that pd-Tempone orients with the plane of the ring perpendicular to the long axis of the lipids. Thus, it is likely that the probe is not dissolved in the hydrocarbon portion of the lipid;[39] pd-Tempone may be located at the lipid–water interface[40] or in the choline head group region in EL, which has been shown to be perpendicular to the lipid chain axis.[41a] In an experiment in the presence of Ni^{2+} we calculate $S_{xx} = -0.031$, $S_{yy} = -0.015$, and $S_{zz} = 0.046$. Thus, the paramagnetic ions perturb EL and change the degree of ordering of the probe.[41b] This is further indication that lipid-dissolved pd-Tempone is located in (or near) the head group region of the bilayers.

For Tempo in EL in the presence of Ni^{2+} the degree of ordering is much less than for pd-Tempone as $a(0\ °C) \simeq a(90\ °C)$. The difference between the h and r parameters at 0 and 90 °C (Table III) suggests that there is some ordering ($|S_{zz}| \leq 0.003$) even in the presence of paramagnetic ions.

Probe Location and Probe Solubility. The line-width parameters A are indicative of probe–probe interactions, either dipolar or Heisenberg exchange. The larger the values of A, the greater the interaction, and hence the greater the local concentration of probe. Using the A parameters as a criterion, Tempo and pd-Tempone are more soluble in fatty acids than in octadecane[38] at temperatures above the melting point of the solvents. This enhanced solubility may be due to favorable interactions between the polar ends of the probes and the polar carboxyl groups of the fatty acids. Tempo was considerably more soluble in oleic than in decanoic acid, presumably due to the presence of the double bond in the former, at the temperatures studied. Below the melting points of the fatty acids an increase in hyperfine splitting of 0.3 G was observed for both probes, suggestive of a location for the probes in the solid state that is closer to the polar carboxyl groups.

The high solubility of the probes in liquid-crystalline saturated phospholipids such as DPL, and the apparent absence of exchange, might be due to their preferential location in the polar region of the membranes, or to a different packing of the hydrocarbon region, or both. In addition, comparison of the hyperfine splittings for Tempo in phospholipids (at temperatures above the phase transition) and in fatty acids (Table I) suggests that the average polarity experienced is the same in both; in contrast, pd-Tempone is apparently located in a somewhat more polar region in phospholipids than in fatty acids. In the phospholipids at temperatures above the phase transition the τ_C/τ_B ratio is not as large as that observed in the hydrocarbons (Table V), suggesting that the probe is not exclusively located in the hydrocarbon region of the former. We suggest that the probe is preferentially located in the polar part of the lipids or in the upper part of the acyl chains where the ordering does not vary appreciably with distance from the carboxyl carbon.[43] The fact that $\tau_C/\tau_B > 1$ (Table V) suggests that Tempo is not aligned with the N–O bond parallel to the long axis of the lipid since in this case model simulations show $\tau_C/\tau_B < 1$.

An increase in the hyperfine splitting similar to that observed in the fatty acids also occurred upon passage through the phase transition of DPL and can be ascribed to the same effect—probe migration to a more polar region.

Dix[5e] found that the relaxation enhancement of the ^{13}C T_1's in DPL at 52 °C due to the probe DTBN was more like that resulting from a head group labeled spin probe than that caused by fatty acid probes labeled at C-5 and C-12.[47] Tempo was found to broaden the methylene envelope to a greater extent than the resonances due to choline methyl in a ^1H NMR study of EL.[48] However, Levine et al.[49] found that the ^1H T_1

relaxation enhancement from a head group labeled probe was larger for the methylene envelope than for the choline methyl groups. The NMR results suggest that Tempo is distributed throughout the membrane, diffuses rapidly within the membrane in the fluid phase, and is preferentially distributed near the polar region of the membrane. Also, in the presence of paramagnetic ions, about 75% of the signal expected for Tempo in lipid is unobservable, probably due to location of the probe very close to the aqueous phase.

V. Conclusions

1. Changes in slope of plots of partitioning parameters as a function of temperature may not only be due to changes in probe concentration in lipid and aqueous phases. Differences in activation energies for probe motion in the two media will affect differently the line widths of the high-field resonances in the spectra of the probes in lipid and in water, introducing errors in the partition parameter calculated from line heights. Sharp breaks in the above plots usually correspond to a true change in state, and probably in partitioning[50] as well.

2. The hyperfine splittings and τ_C/τ_B ratios of Tempo are similar in phospholipids and fatty acids and different in hydrocarbons. This is taken as an indication that the probe is preferentially located near (or in) the polar head region of phospholipids and fatty acids, but does not exclude the possibility that some of the probe molecules are located in the hydrocarbon region of phospholipid bilayers and that diffusion between different regions is rapid. Thus, exchange within the fluid phase of the membrane is fast, whereas exchange between the membrane and the aqueous phase is slow.

3. The results with Tempo also indicate that phospholipids are more viscous than fatty acids and hydrocarbons, and that the probe undergoes a small but significant degree of ordering in phospholipids. Additionally, a distribution of the probes in different sites within the membrane is proposed to contribute to the spectra of Tempo in gel phase DPL.

4. The use of paramagnetic ions to remove the signal due to a spin probe in the aqueous medium results in spectra that allow measurement of g values and hyperfine splittings for the probe in lipid, as well as calculation of τ values. Paramagnetic ions are of questionable value for the determination of the probe concentration in lipids, since ca. 75% of the signal expected for Tempo in lipid was lost, and no information about the motion and ordering of this invisible fraction of the probe could be obtained.

5. The use of Tempone to measure microviscosities is questioned since this probe is ordered in phospholipid membranes, introducing an error in the calculation of τ values from EPR spectra. In addition, the much smaller size of the probe compared to the phospholipid molecules does not yield τ values representative of the true viscosity of the medium.

Acknowledgments. S.S. is grateful to the Exchange Program between the National Research Council of Canada and the Conselho Nacional de Desenvolvimento Cientifico e Tecnológico (Brazil) for a fellowship. We thank Michael Taylor for obtaining some of the EPR spectra.

References and Notes

(1) (a) Issued as N.R.C.C. No. 17142. (b) Veterans' Administration Hospital, Minneapolis, Minn. 55417. (c) On leave from Department of Biochemistry, Institute of Chemistry, University of São Paulo, C.P. 20.780, São Paulo, Brazil.
(2) E. J. Shimshick and H. M. McConnell, *Biochemistry,* **12** 2351–2360 (1973); *Biochem. Biophys. Res. Commun.,* **53,** 446–451 (1973).
(3) C. D. Linden, K. L. Wright, H. M. McConnell, and C. F. Fox, *Proc. Natl. Acad. Sci. U.S.A.,* **70,** 2271–2275 (1973); S. H. W. Wu and H. M. McConnell, *Biochemistry,* **14,** 847–854 (1974); W. Kleemann, C. W. M. Grant, and H. M. McConnell, *J. Supramol. Struct.,* **2,** 609–616 (1974); W. Kleeman and H. M. McConnell, *Biochim. Biophys. Acta,* **419,** 206–222 (1976); H. M. McConnell in "Spin Labeling Theory and Applications", L. J. Berliner, Ed., Academic Press, New York, N.Y., 1976, pp 525–560; E. J. Luna and H. M. McConnell, *Biochim. Biophys. Acta,* **466,** 381–392 (i977).
(4) C. D. Linden, A. D. Keith, and C. F. Fox, *J. Supramol. Struct.,* **1,** 523–534 (1973); B. J. Wisnieski, J. G. Parkes, Y. O. Huang, and C. F. Fox, *Proc. Natl. Acad. Sci. U.S.A.,* **71,** 4381–4385 (1974); C. F. Fox in "Biochemistry of Cell Walls and Membranes", C. F. Fox, Ed., University Park Press, Baltimore, Md., 1975, pp 279–306; B. J. Wisnieski and K. K. Iwata, *Biochemistry,* **16,** 1321–1326 (1977).
(5) (a) J. A. Dix, J. M. Diamond, and D. Kivelson, *Proc. Natl. Acad. Sci. U.S.A.,* **71,** 474–478 (1974); (b) J. K. Lanyi, W. Z. Plachy, and M. Kates, *Biochemistry,* **13,** 4914–4920 (1974); (c) M. Tomkiewicz and G. A. Corker, *Biochim. Biophys. Acta,* **406,** 197–205 (1976); (d) Z. Novosad, R. D. Knapp, A. M. Gotto, H. J. Pownall, and J. D. Morrisett, *Biochemistry,* **15,** 3176–3183 (1976); (e) J. A. Dix, Ph.D. Thesis, UCLA, Los Angeles, Calif., 1977.
(6) E. Sackmann, H. Träuble, H. J. Galla, and P. Overath, *Biochemistry,* **12,** 5360–5369 (1973); A. D. Keith, M. Sharnoff, and G. E. Cohn, *Biochim. Biophys. Acta,* **300,** 379–419 (1973).
(7) W. L. Hubbell and H. M. McConnell, *Proc. Natl. Acad. Sci. U.S.A.,* **61,** 12–16 (1968).
(8) Resolution of all three nitrogen hyperfine lines has been accomplished in experiments done at a higher frequency (35 GHz); (a) O. H. Griffith, L. J. Libertini, and G. B. Birrell, *J. Phys. Chem.,* **75,** 3417–3425 (1971); (b) B. J. Gaffney in "Methods in Enzymology", Vol. 32B, S. Fleischer and L. Packer, Eds., Academic Press, New York, N.Y., 1974, pp 161–197, and by using perdeuterated DTBN at 9.5 GHz; (c) W. Z. Plachy and D. A. Windrem, *J. Magn. Reson.,* **27,** 237–239 (1977).
(9) A. G. Lee, N. J. M. Birdsall, J. C. Metcalfe, P. A. Toon, and G. B. Warren, *Biochemistry,* **13,** 3699–3705 (1974).
(10) T. R. Hesketh, G. A. Smith, M. D. Houslay, K. A. McGill, N. J. M. Birdsall, J. C. Metcalfe, and G. B. Warren, *Biochemistry,* **15,** 4145–4151 (1976).
(11) (a) J. S. Hwang, R. P. Mason, L. P. Hwang, and J. H. Freed, *J. Phys. Chem.,* **79,** 489–511 (1975); (b) C. F. Polnaszek and J. H. Freed, *ibid.,* **79,** 2283–2306 (1975); (c) J. S. Hwang, K. V. S. Rao, and J. H. Freed, *ibid.,* **80,** 1490–1501 (1976); (d) J. H. Freed in "Spin Labeling Theory and Applications", L. J. Berliner, Ed., Academic Press, New York, N.Y., 1976, pp 53–132; (e) C. F. Polnaszek, Ph.D. Thesis, Cornell University, Ithaca, N.Y., 1976.
(12) L. R. Dalton, B. H. Robinson, L. A. Dalton, and P. Coffey, *Adv. Magn. Reson.,* **8,** 149–259 (1976).
(13) (a) A. D. Keith and W. Snipes, *Science,* **183,** 666–668 (1974); (b) P. D. Morse, M. Ruhlig, W. Snipes, and A. D. Keith, *Arch. Biochem. Biophys.,* **168,** 40–56 (1976); (c) S. A. Henry, A. D. Keith, and W. Snipes, *Biophys. J.,* **16,** 641–653 (1976); (d) A. D. Keith, W. Snipes, and D. Chapman, *Biochemistry,* **16,** 634–641 (1977).
(14) (a) J. H. Freed and G. K. Fraenkel, *J. Chem. Phys.,* **39,** 326–348 (1963); (b) J. H. Freed, *ibid.,* **41,** 2077–2083 (1964).
(15) (a) S. A. Goldman, G. V. Bruno, C. F. Polnaszek, and J. H. Freed, *J. Chem. Phys.,* **56,** 716–735 (1972); (b) C. F. Polnaszek, *Q. Rev. Biophys.,* submitted.
(16) E. G. Rozantsev, "Free Nitroxyl Radicals", Plenum Press, New York, N.Y., 1970.
(17) F. Daniels, J. W. Williams, P. Bender, R. A. Alberty, and C. D. Cornwell, "Experimental Physical Chemistry", 6th ed., McGraw-Hill, New York, N.Y., 1962, pp 147–157.
(18) I. C. P. Smith and K. W. Butler in "Spin Labeling Theory and Applications", L. J. Berliner, Ed., Academic Press, New York, N.Y., 1976, pp 411–451.
(19) We have used non-SI units; the appropriate conversions are 1 G = 0.1 mT, 1 cal = 4.814 J, 1 P = 0.1 Pa·s, 1 Å = 0.1 nm.
(20) The high field line due to the probe in lipid (Fig. 1) can broaden considerably upon going below the phase transition and, in some cases, there can be overlap of the high-field portion of the $m_I = -1$ line of the probe in lipid with the corresponding peak of the probe in water. Then the intensity at P will not be due solely to the probe in aqueous media and the apparent f parameter will be smaller than its actual value.
(21) B. Cannon, C. F. Polnaszek, K. W. Butler, L. G. Eriksson, and I. C. P. Smith, *Arch. Biochem. Biophys.,* **167,** 505–516 (1975).
(22) J. D. Castle and W. L. Hubbell, *Biochemistry,* **15,** 4818–4831 (1976).
(23) J. H. Freed, G. V. Bruno, and C. F. Polnaszek, *J. Phys. Chem.,* **75,** 3385–3399 (1973); C. F. Polnaszek, G. V. Bruno, and J. H. Freed, *J. Chem. Phys.,* **58,** 3185–3199 (1973); M. J. Neal, K. W. Butler, C. F. Polnaszek, and I. C. P. Smith, *Mol. Pharmacol.,* **12,** 144–155 (1976).
(24) (a) R. Brière, H. Lemaire, A. Rassat, P. Rey, and A. Rousseau, *Bull. Soc. Chim. Fr.,* 4479–4484 (1967); (b) A. Rassat in "Molecular Spectroscopy", P. Hepple, Ed., Institute of Petroleum, London, 1968, pp 145–155; (c) A. Rassat, *Pure Appl. Chem.,* **25,** 623–634 (1971).
(25) C. Jolicoeur and H. L. Friedman, *Ber. Bunsenges. Phys. Chem.,* **75,** 248–257 (1971); *J. Solution Chem.,* **3,** 15–43 (1974).
(26) C. C. Whisnant, S. Ferguson, and D. B. Chestnut, *J. Phys. Chem.,* **78,** 1410–1415 (1974); G. Poggi and C. S. Johnson, *J. Magn. Reson.,* **3,** 436–445 (1971).
(27) K. W. Butler, N. H. Tattrie, and I. C. P. Smith, *Biochim. Biophys. Acta,* **363,** 351–360 (1974); H. Utsumi, K. Inone, S. Najima, and T. Kwan, *Chem. Pharm. Bull.,* **24,** 1219–1225 (1976).
(28) B. J. Gaffney and S. C. Chen in "Methods in Membrane Biology", Vol. 8, E. D. Korn, Ed., Plenum Press, New York, N.Y., 1977, pp 291–358.
(29) G. I. Likhtenshtein, "Spin Labeling Methods in Molecular Biology", Wiley-Interscience, New York, N.Y., 1976.
(30) F. A. Cotton and G. A. Wilkinson, "Advanced Inorganic Chemistry", 3rd ed., Interscience, New York, N.Y., 1972, p 52.
(31) D. Chapman, W. E. Peel, B. Kingston, and T. H. Lilley, *Biochim. Biophys. Acta,* **464,** 260–275 (1977).
(32) H. Schindler and J. Seelig, *J. Chem. Phys.,* **59,** 1841–1850 (1973); **61,** 2946–2949 (1974).
(33) R. C. Weast, Ed., "Handbook of Chemistry and Physics", 57th ed., The Chemical Rubber Publishing Co., Cleveland, Ohio, 1976.
(34) W. Z. Plachy and D. Kivelson, *J. Chem. Phys.,* **47,** 3312–3318 (1967); M. P. Eastman, R. G. Kooser, M. R. Das, and J. H. Freed, *J. Chem. Phys.,* **51,** 2690–2709 (1969); P. Devaux, C. J. Scandella, and H. M. McConnell, *J. Magn. Reson.,* **9,** 474–485 (1973).

(35) S. Schreier-Muccillo, K. W. Butler, and I. C. P. Smith, *Arch. Biochem. Biophys.*, **159**, 297–311 (1973).
(36) It is unfortunate that it is the high field lines which are resolved. The variation of the height of the $m = -1$ line with τ is greater than that for the other two lines. In systems where all three lines are resolved,[8] one may get different results as a function of temperature by calculating f or α for each line.
(37) P. Tancrède, P. Bothorel, P. de St. Romain, and D. Patterson, *J. Chem. Soc., Faraday Trans. 2*, **73**, 15–28 (1977); P. Tancrède, P. Bothorel, and D. Patterson, *ibid.*, 29–39 (1977).
(38) S. Zager and J. H. Freed (unpublished results) have found that pd-Tempone is not very soluble in a series of long-chain *n*-alkanes.
(39) In nematic phase 7-A pd-Tempone and Tempo were found to align with the plane of the ring tending to be parallel to the long axes of the solvent molecules.
(40) M. Setaka and C. Lagercrantz, *J. Am. Chem. Soc.*, **97**, 6013–6018 (1975).
(41) (a) J. Seelig, H. U. Gally, and R. Wohlgemuth, *Biochim. Biophys. Acta*, **467**, 109–119 (1977); (b) M. F. Brown and J. Seelig, *Nature (London)*, **269**, 721–723 (1977).
(42) B. R. Lentz, Y. Barenholz, and T. E. Thompson, *Biochemistry*, **15**, 4521–4528 (1976).
(43) G. W. Stockton, C. F. Polnaszek, A. P. Tulloch, F. Hasan, and I. C. P. Smith, *Biochemistry*, **15**, 954–966 (1976); A. Seelig and J. Seelig, *ibid.*, **13**, 4839–4844 (1974).
(44) D. Marsh, A. Watts, and P. F. Knowles, *Biochim. Biophys. Acta*, **465**, 500–514 (1977).
(45) J. Suurkuusk, B. R. Lentz, Y. Barenholz, R. Biltonen, and T. E. Thompson, *Biochemistry*, **15**, 1393–1401 (1976).
(46) M. Windholz, Ed., "The Merck Index", 9th ed., Merck and Co. Inc., Rahway, N.J., 1976.
(47) Y. K. Levine, N. J. M. Birdsall, A. G. Lee, and J. C. Metcalfe, *Biochemistry*, **11**, 1416–1421 (1972).
(48) L. O. Sillerud and R. E. Barnett, *Biochim. Biophys. Acta*, **465**, 466–470 (1977).
(49) Y. K. Levine, A. G. Lee, N. J. M. Birdsall, J. C. Metcalfe, and J. D. Robinson, *Biochim. Biophys. Acta*, **291**, 592–607 (1973).
(50) Y. Katz and J. M. Diamond, *J. Membrane Biol.*, **17**, 101–120 (1974).
(51) NOTE ADDED IN PROOF: J. A. Dix, D. Kivelson, and J. M. Diamond, *J. Membrane Biol.*, **40**, 315–342 (1978), have recently examined the partitioning of DBTN in DPL bilayers.

Effects of Donor Molecules on the Palladium-Catalyzed Cyclocotrimerization of Acetylenes with Olefins. Preparation of Dimeric Tetrakis(methoxycarbonyl)palladiacyclopentadiene(base) Complexes and the Structure with Base = 2,6-Lutidine

Leo D. Brown,[1a] Kenji Itoh,*[1b] Hiroharu Suzuki,[1b] Kenji Hirai,[1b] and James A. Ibers*[1a]

Contribution from the Department of Chemistry, Northwestern University, Evanston, Illinois 60201, and the Department of Synthetic Chemistry, Faculty of Engineering, Nagoya University, Furo-cho, Chikusa, Nagoya 464, Japan.
Received May 12, 1978

Abstract: A tetrakis(methoxycarbonyl)cyclohexadiene annulation of norbornene, cyclopentene, and cyclohexene with two molecules of dimethyl acetylenedicarboxylate (DMAD) is effectively catalyzed by a combination of an oligomeric palladiacyclopentadiene complex, $[Pd(C_4(COOCH_3)_4)]_n$ (**1**), with 1 equiv of triphenylphosphine. The reaction of **1** with L = pyridine, α-picoline, 2,5-lutidine, 2,6-lutidine, or triphenylphosphine led to new dimeric complexes of formula $[Pd(C_4(COOCH_3)_4)L]_2$. In these complexes there is intermolecular coordination through the carbonyl oxygen atom of the α-methoxycarbonyl group as deduced from spectroscopic results and as shown in an X-ray structure determination of the L = 2,6-lutidine complex. This complex crystallizes with four dimers in space group C_{2h}^5-$P2_1/c$ of the monoclinic system in a cell of dimensions a = 16.967 (4) Å, b = 14.362 (3) Å, c = 18.410 (5) Å, β = 112.05 (1)°. The structure has been refined by full-matrix least-squares methods to values of R and R_w of 0.036 and 0.050, respectively, based on 440 variables and 8287 observations. Acceleration of the rate of cyclocotrimerization of two DMAD molecules with norbornene by the addition of 1 equiv of triphenylphosphine to the catalyst, **1**, and the formation of the dimeric complex are explained in terms of a common three-coordinate intermediate, "$Pd(C_4(COOCH_3)_4)L$", which is effectively trapped by an entering cycloolefin in the palladium-catalyzed cyclohexadiene annulation.

Metallocycles have attracted considerable interest because they are often key intermediates in various homogeneous catalytic reactions. For example, metallocyclobutane is an important intermediate in olefin metathesis,[2] transition metal mediated $[\sigma 2 + \sigma 2]$ skeletal isomerization,[3] and $[\sigma 2 + \pi 2]$ cycloadditions[4] of strained molecules, Metallocyclopentadiene complexes, $[MC_4R_4]L_n$, are key intermediates in cyclooligomerization[5-9] or cyclocooligomerization[10-16] of various acetylenes using low-valent transition-metal catalysts. Recently we reported that tetrakis(methoxycarbonyl)palladiacyclopentadiene cyclic olefin complexes are key intermediates for a formally $[\pi 2 + \pi 2 + \pi 2']$ cyclocooligomerization between two molecules of dimethyl acetylenedicarboxylate (DMAD) and an electron-donating olefin, such as norbornene (NB) or norbornadiene.[16] The oligomeric $[Pd(C_4(COOCH_3)_4)]_n$ (**1**) species is a catalyst for the cyclocotrimerization of two DMAD molecules with one NB molecule (eq 1). The reaction proceeds

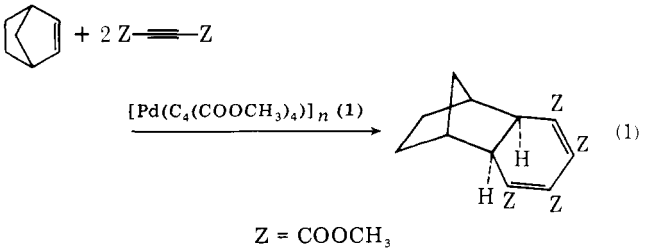

(1)

Z = $COOCH_3$

without formation of hexamethyl mellitate, the cyclotrimerization product of three molecules of DMAD. A plausible mechanism[16] of this palladium-catalyzed cyclocotrimerization reaction is shown in Scheme I, where L is DMAD or a cyclic olefin present as a reactant in the catalytic system.

We have now found that the rate of reaction 1 is markedly increased, after a slight induction period, if triphenylphosphine

0002-7863/78/1500-8232$01.00/0